Electronic Supplementary Material (ESI) for Polymer Chemistry.
This journal is © The Royal Society of Chemistry 2023

Electronic Supporting information

Synthesis of cRGD peptide cluster-decorated NIR-fluorescent PISA-RAFT nanoparticles targeting integrin expressing cells

Damien Duret,[a] Adrien Grassin,[b] Maxime Henry,[c] Pierre Alcouffe,[a] Sebastian Raja,[d] Carlos Baleizao,[d] José Paulo Farinha,[d] Marie-Thérèse Charreyre,[a] Didier Boturyn,[b] Jean-Luc Coll,[c] Arnaud Favier[a]

[a] Université de Lyon, CNRS, Université Lyon 1, INSA Lyon, Université Jean Monnet, UMR 5223, Ingénierie des Matériaux Polymères, F-69621 Villeurbanne, France.

[b] University Grenoble Alpes, CNRS, UMR 5250, Department of Molecular Chemistry, 38000 Grenoble, France.

[c] University Grenoble Alpes, Institute for Advanced Biosciences, Team Cancer Targets and Experimental Therapeutics, INSERM U1209, CNRS UMR5309, Grenoble 38100, France.

[d] Centro de Química Estrutural, Institute of Molecular Sciences and Department of Chemical Engineering, Instituto Superior Técnico, University of Lisbon, P-1049-001 Lisbon, Portugal.

PISA-RAFT experiments.

Table S1. Details PISA-RAFT experiments

Exp.	Solvent	MacroCTA	CTA/ ACPA	BDA (mol% vs. nBA)	Fluorescent monomer (mol% vs. nBA)	Time (h)	Conv. (%)	QELS D_h (sd)	PDI
1	H_2O	PNAM	5	0	0	27	89	42 (17)	0.20
2			3			21	80	48 (18)	0.17
3			2.5			5	93	62 (25)	0.19
4			2			2	97	68 (23)	0.15
5	H_2O/CH_3CN 50 vol%	PNAM	2.5	0	0	1.5 2.5 3.5 4.5 20	40 58 71 78 83	34 (9) 45 (13 50 (14) 51 (17) 59 (19	0.15 0.18 0.15 0.12 0.18
6	H_2O/CH_3CN 50 vol%	PNAM	2.5	1.5	0	6	86	59 (19)	0.21
7				3		6	81	42 (11)	0.10
8				6		6	86	38 (10)	0.11
9				9		6	92	58 (18)	0.16
10				12		6	91	gel	n/a
11	H_2O/CH_3CN 50 vol%	PNAM	2.5	3	PDI-BisMAm 0.15	6	67	36 (11)	0.19
NP1	H_2O/CH_3CN 50 vol%	PNAM	2.5	3	Cy5.5-Am 0.15	6	85	47 (10)	0.15
NP2	H_2O/CH_3CN 50 vol%	PNAM + Peptide-PNAM 2.5 mol%	2.5	3	0	6	83	52	0.12
NP3	H_2O/CH_3CN 50 vol%	PNAM + Peptide-PNAM 2.5 mol%	2.5	3	Cy5.5-Am 0.15	6	58	63 (27)	0.18

Synthesis of PDI-BisMAm NIR-fluorescent crosslinker.

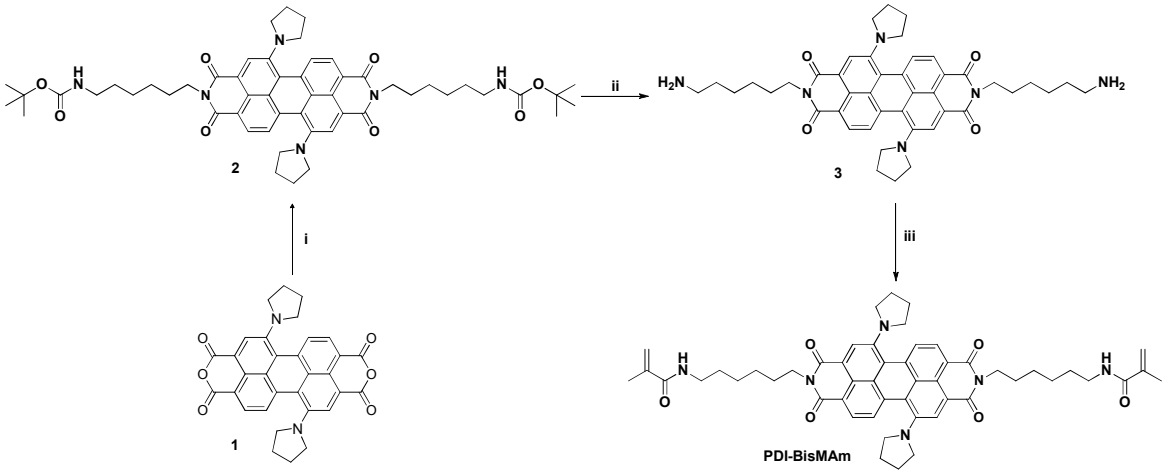

Scheme S1. Synthesis of PDI PDI-BisMAm NIR-fluorescent crosslinker. Reagents and conditions: i) *N*-Boc-1,6-hexanediamine, NEt_3, DMF, 100°C, 48 h. ii) CF_3COOH, DCM, 0°C, 12 h; iii) methacryloyl chloride, TEA, toluene, 12 h.

***N,N'*-Bis[(amino-hexyl)-6-carbamic acid tert-butyl ester]-1,7-bis(pyrrolidyn-1-yl)perylene-3,4:9,10-tetracarboxylic acid bisimide** (2)**.** A mixture of 1,7-dipyrrolidinylperylene-3,4:9,10-tetracarboxylic acid bisanhydride (1) (0.04 g, 0.07 mmol), *N*-Boc-1,6-hexanediamine (0.08g, 0.36 mmol), synthesized as described in the literature,[1]and NEt_3 (0.04g, 0.43 mmol) in DMF (15 mL) were added into a round-bottom flask. The reaction mixture was stirred in an argon atmosphere at 100 °C for 48 h. After completion of the reaction, the mixture was washed with dichloromethane (3×100 mL) and water (1×50) mL. The organic phase was evaporated and a flash column chromatography was used with a 10:9:1 ratio of dichloromethane / ethylacetate / methanol to afford the final compound (2) as a greenish solid in 79% yield.

^{1}H NMR (300 MHz,$CDCl_3$): δ 1.42 (s, 28H); 1.74 (s, 4H); 1.95-2.02 (m, 8H); 2.75 (s, 4H); 3.09-3.11 (m, 4H); 3.68 (s, 4H); 4.21 (t, *J* = 7.2 Hz, 4H); 4.59 (s, 2H); 7.54 (d, *J* = 8.1 Hz, 2H); 8.32 (d, *J* = 8.1 Hz, 2H); 8.36 (s, 2H); ^{13}C NMR (75 MHz, $CDCl_3$): δ 25.9, 26.6, 26.7, 28.2, 28.6, 30.1, 31.1, 40.4, 40.6, 52.3, 79.1, 118.1, 119.1, 120.8, 121.7, 122.2, 123.9, 126.7, 129.9, 134.3, 146.6, 156. 1, 164.2. HRMS (ESI): m/z for $C_{54}H_{66}N_6O_8$ calcd. 926.4942; found 927.4987 (M^++H).

***N,N'*-Bis(6-aminohexane)1,7-dipyrrolidynylperylene-3,4:9,10-tetracarboxylic acid bisimide** (3)**.** Compound (2) (0.04g, 0.04 mmol) was dissolved in dichloromethane (6 ml) and TFA (0.25 ml) was added drop-wise. The reaction mixture was stirred for 12 hours, at 0 °C. Then, the reaction mixture was poured into ice and neutralized carefully with NH_3 (solution at 10%) until pH 8. The residue was extracted with dichloromethane, washed with brine, dried over Na_2SO_4 and evaporated to obtain the desired product (3) as a greenish solid in 57% yield. ^{1}H NMR (300 MHz, $CDCl_3$): δ 1.43 (s, 8H); 1.76-1.80 (m, 8H); 1.93-1.98 (m, 8H); 2.66-2.70 (m, 8H); 3.64 (s, 4H); 4.20 (t, *J* = 7.5 Hz, 4H); 7.47 (d, *J* = 7.8 Hz, 2H); 8.28 (d, *J* = 8.1 Hz, 2H); 8.33 (s, 2H). ^{13}C NMR (75 MHz, $CDCl_3$): δ 25.7, 26.5, 26.9, 28.0, 33.5, 40.3, 42.0, 52.1, 117.8, 118.8, 120.6, 121.5, 121.9, 123.6, 126.5, 129.7, 134.0, 146.3, 164.0.

***N*,*N'*-Bis[(amino-hexyl)-6-methacrylamide]-1,7-bis(pyrrolidyn-1-yl)perylene-3,4:9,10-tetracarboxylic acid bisimide** (4)**.** Compound (3) (0.04, mmol) and methacryloyl chloride (0.04, mmol) were dissolved in toluene (10 ml). The reaction mixture was stirred for 12 hours, at room temperature. Then, the residue was extracted with dichloromethane, washed with brine, dried over Na_2SO_4 and evaporated to obtain the desired product (4) as a greenish solid in 73% yield.

^{1}H NMR (300 MHz, $CDCl_3$): δ 1.37-1.76 (m, 20H); 1.96 (s, 6H); 2.68 (s, 4H); 3.09-3.10 (m, 4H); 3.27-3.31 (m, 4H); 3.61 (s, 4H); 4.20 (t, *J* = 6.6 Hz, 4H); 5.29 (s, 2H); 5.70 (s, 2H); 6.16 (s, 2H); 7.40 (d, *J* = 7.8 Hz, 2H); 8.21-8.24 (m, 4H); ^{13}C NMR (75 MHz, $CDCl_3$): δ 8.6, 18.7, 25.7, 26.4, 26.5, 27.9, 29.3, 29.6, 39.4, 40.0, 45.8, 52.0, 117.7, 118.7, 119.1, 120.5, 121.3, 121.8, 123.5, 126.4, 129.5, 133.8, 140.2, 146.2, 163.9, 168.4. HRMS (ESI): m/z for $C_{52}H_{58}N_6O_6$ calcd. 862.4418; found 863.4472 (M^+).

Purification of the cRGDcluster-CTA.

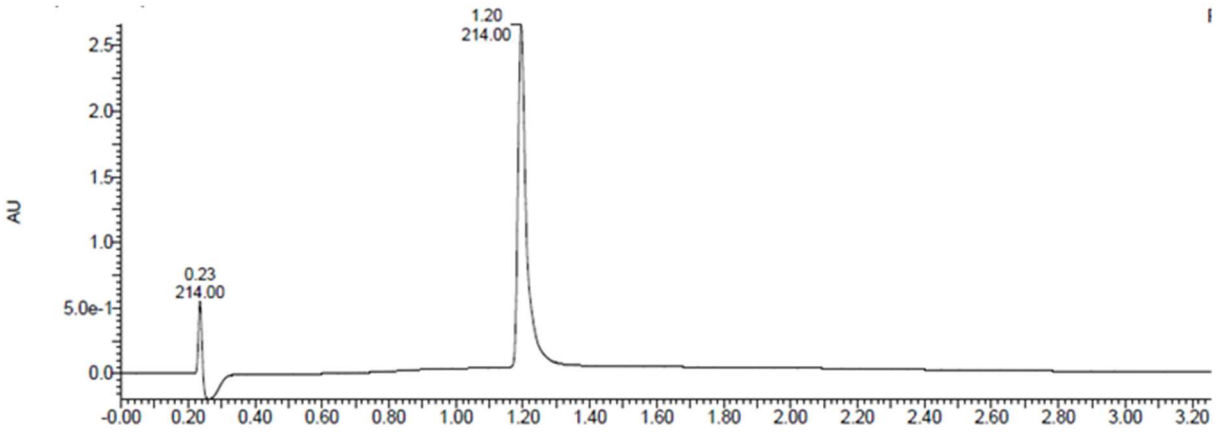

Figure S1. RP-UHPLC chromatogram of the purified cRGDcluster-CTA (λ = 214 nm)

NMR spectra.

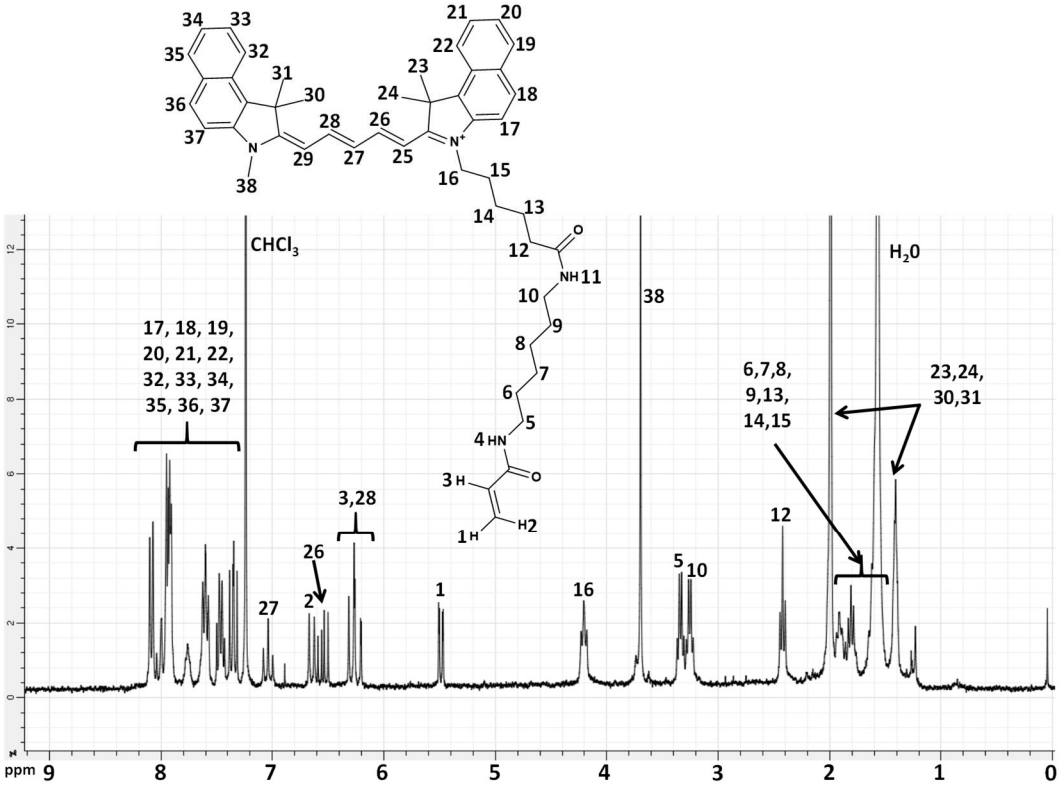

Figure S2. ^{1}H NMR spectrum of the purified Cy5.5-Am monomer in $CDCl_3$

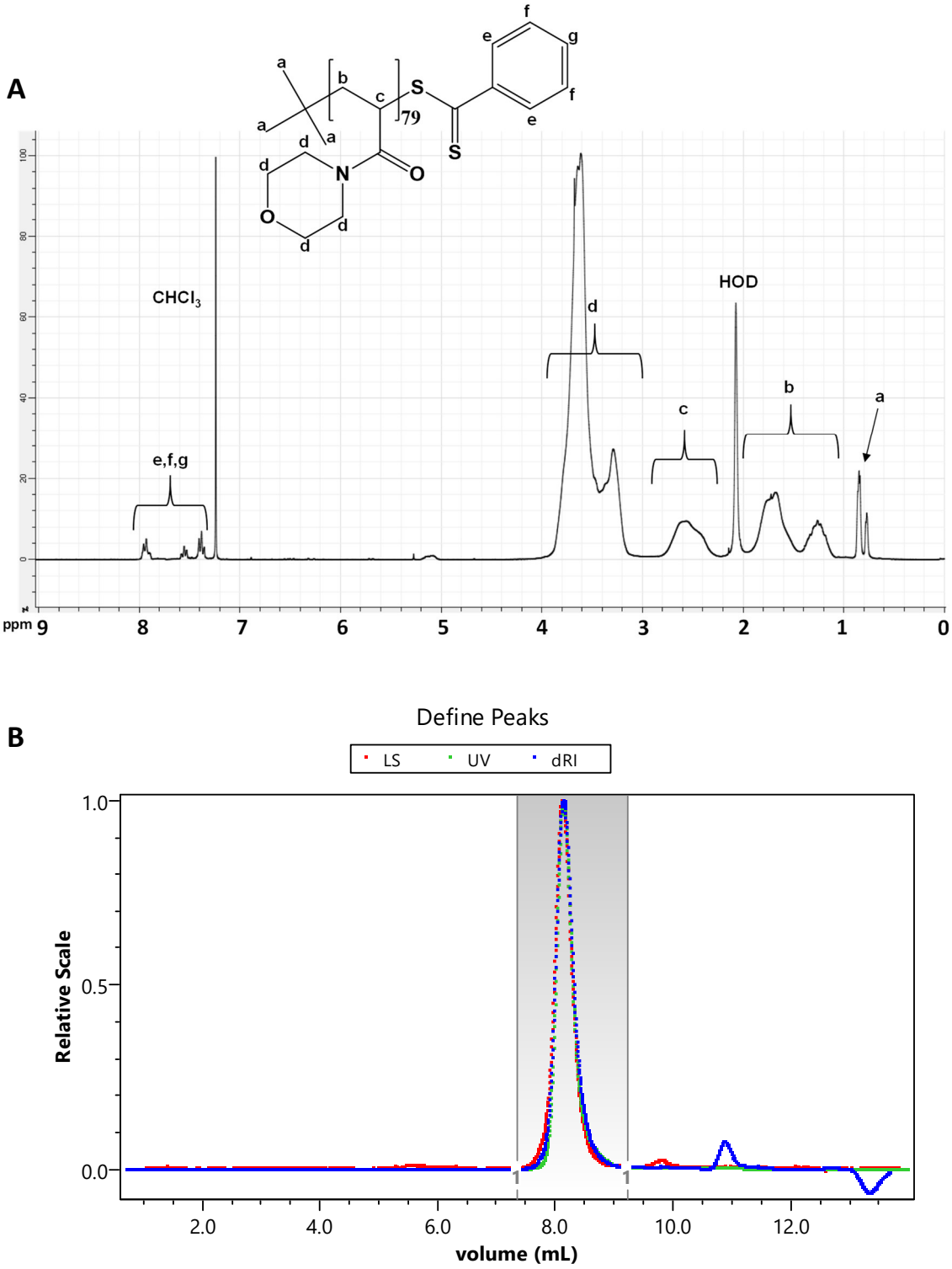

Figure S3. ^{1}H NMR spectrum in $CDCl_3$ (A) and SEC-MALLS analysis (B) of PNAM-CTA prepared by RAFT polymerization in the presence of tert-butyl dithiobenzoate CTA. Protons corresponding to the polymer chain-ends were clearly observed on the NMR spectrum and SEC-MALLS chromatograms showed a very narrow distribution (M_n = 11 300 g.mol^{-1}, Đ = 1.03), as demonstrated by the overlapping of the peaks detected by a multi-angle light scattering detector (red), a UV detector set at 302 nm (absorption band of the dithiobenzoate end-group of the polymer chain) (green) and a refractive index detector (blue). M_n values obtained by both techniques were in very close agreement.[2]

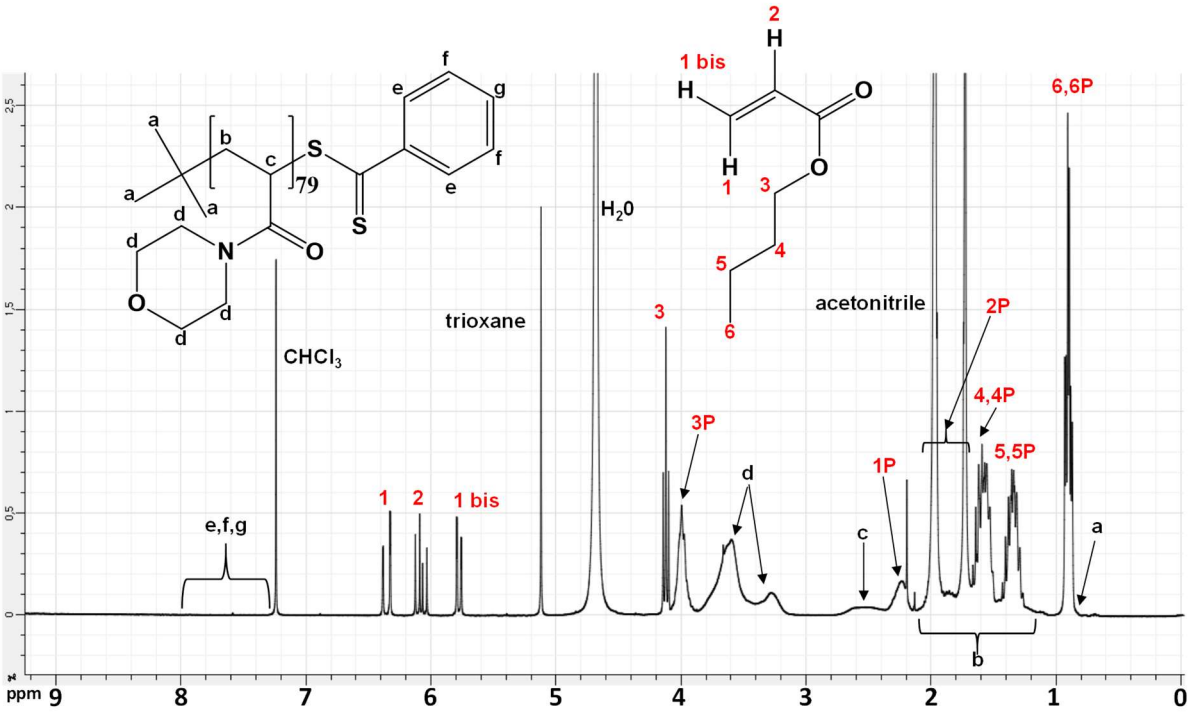

Figure S4. ^{1}H NMR spectrum in $CDCl_3$ of a raw PISA-RAFT sample withdrawn during polymerization of nBA in the presence of the PNAM macroCTA in water/acetonitrile 50vol%.

Table S2. ^{1}H NMR attribution for the cRGDcluster-PNAM macroCTA

Area		cRGDcluster-PNAM macroCTA			
		ppm	Attribution	Number of protons	Observed in D_2O/acetonitrile-d
A (6-9 ppm)		>8	COO**H** (Asp)	$4 \times n_p$	No
		>8	CO-N**H** (peptide amides)	$36 \times n_p$	No
		>8	N**H**-C(=O) (Lys)	$1 \times n_p$	No
		7.5	N**H** (Arg)	$16 \times n_p$	No
		7.5	C**H** (oxime linker)	$4 \times n_p$	Yes
		7.2-7.3	**H**-aromatic (Phe)	$20 \times n_p$	Yes
		7.2-8	**H**-aromatic (ω-dithiobenzoate chain-end)	$5 \times n_p$	Yes
		total		$86 \times n_p$	$\mathbf{29 \times n_p}$
B (3-5.5 ppm)	**D (2.3-5.5 ppm)**	5.2	C**H**-S-C(=S)-Ph	$1 \times n_p$	Yes
		4-5	CO-C**H**-N (peptide)	$24 \times n_p$	Yes
		4.9	CO-C**H$_2$**-O (oxime linker)	$8 \times n_p$	Yes
		4.6	C**H** (squelette ATC)	$1 \times n_p$	Yes
		4.1	CO-C**H$_2$**-N (Gly)	$12 \times n_p$	Yes
		3.76	C**H$_2$** (morpholine NAM)	$8 \times n_{NAM}$	Yes
		3.4	C**H$_2$**-Phenyl (Phe)	$8 \times n_p$	Yes
		2.6-3.5	C**H$_2$**-N (Arg, Lys, Pro)	$28 \times n_p$	Yes
C (0-3 ppm)		2.7-2.9	C**H$_2$**-COOH (Asp)	$8 \times n_p$	Yes
		2.7	C**H** (PNAM backbone)	$1 \times n_{NAM}$	Yes
		2.7	C**H$_2$**-NH-C(=O) (Lys)	$2 \times n_p$	Yes
		total		$9 \times n_{NAM} + 92 \times n_p$	$\mathbf{9 \times n_{NAM} + 92 \times n_p}$
	E (0-2.3 ppm)	1.9-2.3	C**H$_2$** (Pro)	$8 \times n_p$	Yes
		1.9	C**H$_2$** (squelette polymère)	2x	Yes
		1.6-1.8	C**H$_2$** (Arg)	$16 \times n_p$	Yes
		1.2-1.8	C**H$_2$** (Lys)	$54 \times n_p$	Yes
		1.6	C**H$_3$** (squelette ATC)	$3 \times n_p$	Yes
		1.5	C**H$_3$** (Ala)	$3 \times n_p$	Yes
		total		$2 \times n_{NAM} + 84 \times n_p$	$\mathbf{2 \times n_{NAM} + 84 \times n_p}$

n_p = Number of cRGD-peptide-cluster, n_{NAM} = number of NAM units.

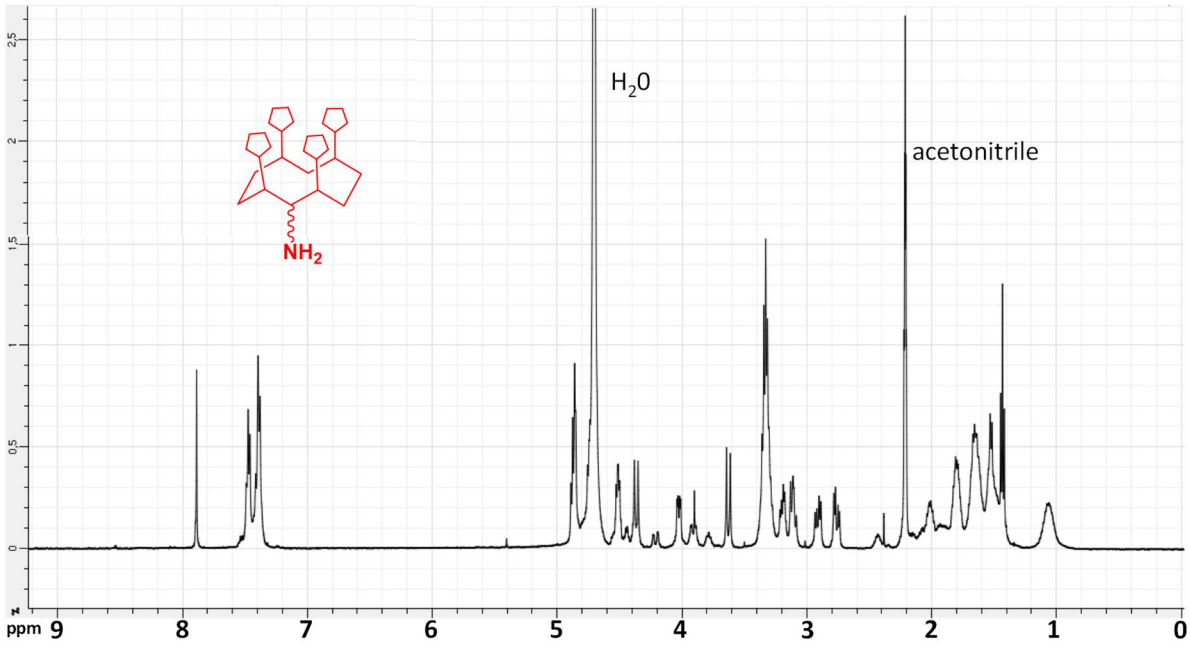

Figure S5. ^{1}H NMR of the free cRGD-peptide-cluster in D_2O/CD_3CN 70/30 vol%.

Kinetics of PISA-RAFT experiments.

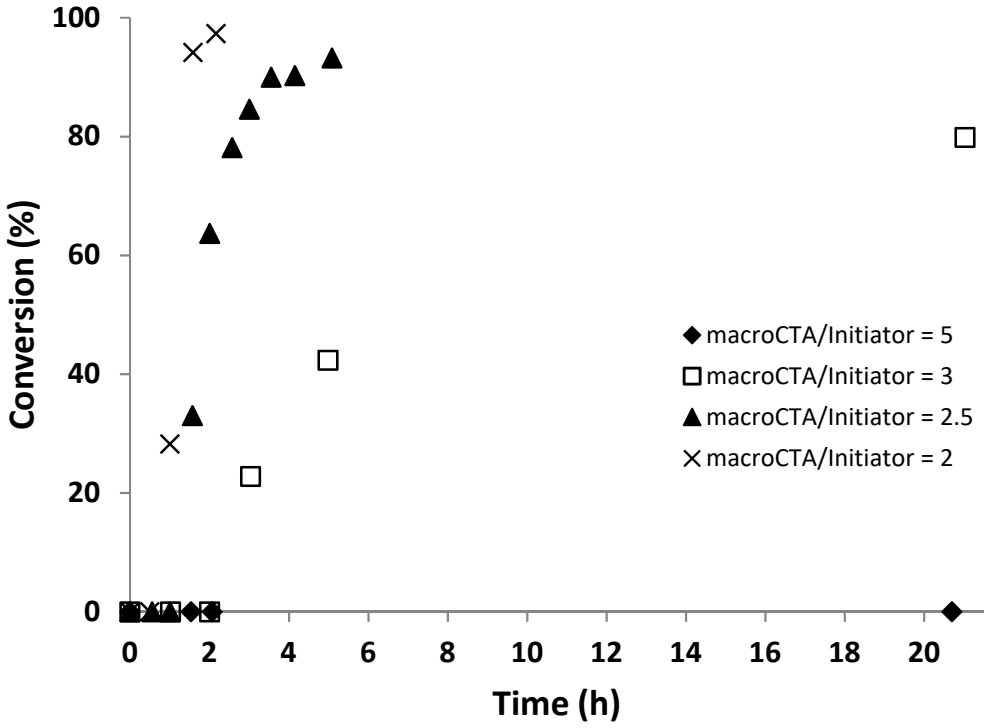

Figure S6. Kinetics of PISA-RAFT experiments at various macroCTA/Initiator ratio (Exp. **1-4** in Table S1). Solvent = Water, initial nBA concentration = 1M and initial molar ratio nBA/macroCTA = 156.3.

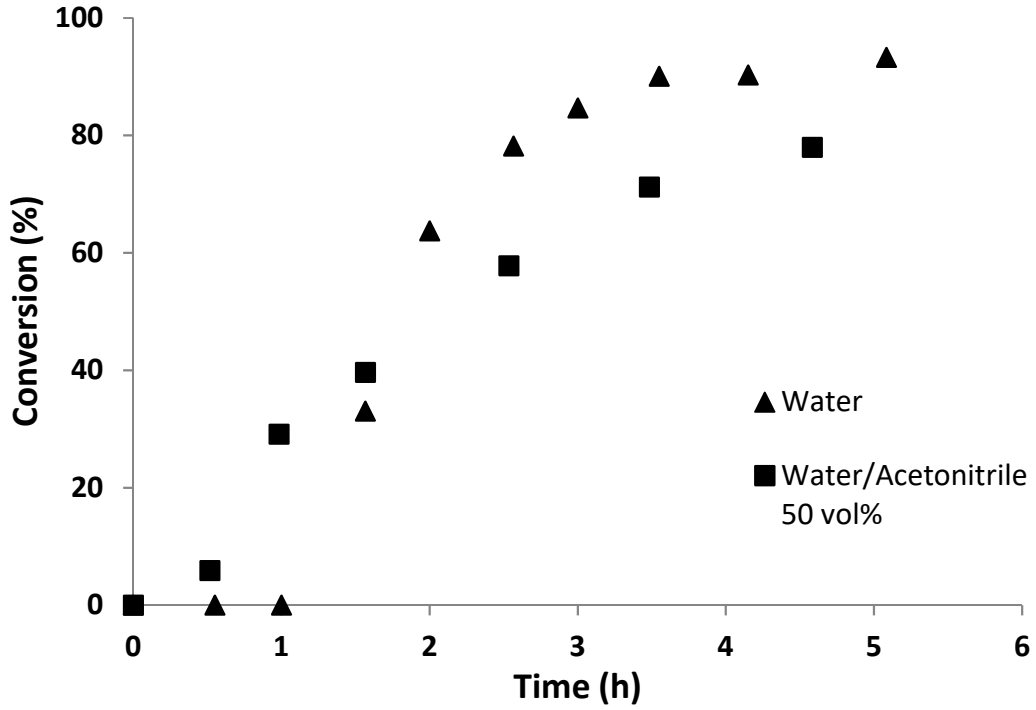

Figure S7. Comparison of PISA-RAFT experiments performed in water and in a mixture water/acetonitrile 50 vol% (Exp. **3** and **5** in Table S1, respectively).

Evolution of the hydrodynamic PISA-RAFT nanoparticle diameter with polymerization.

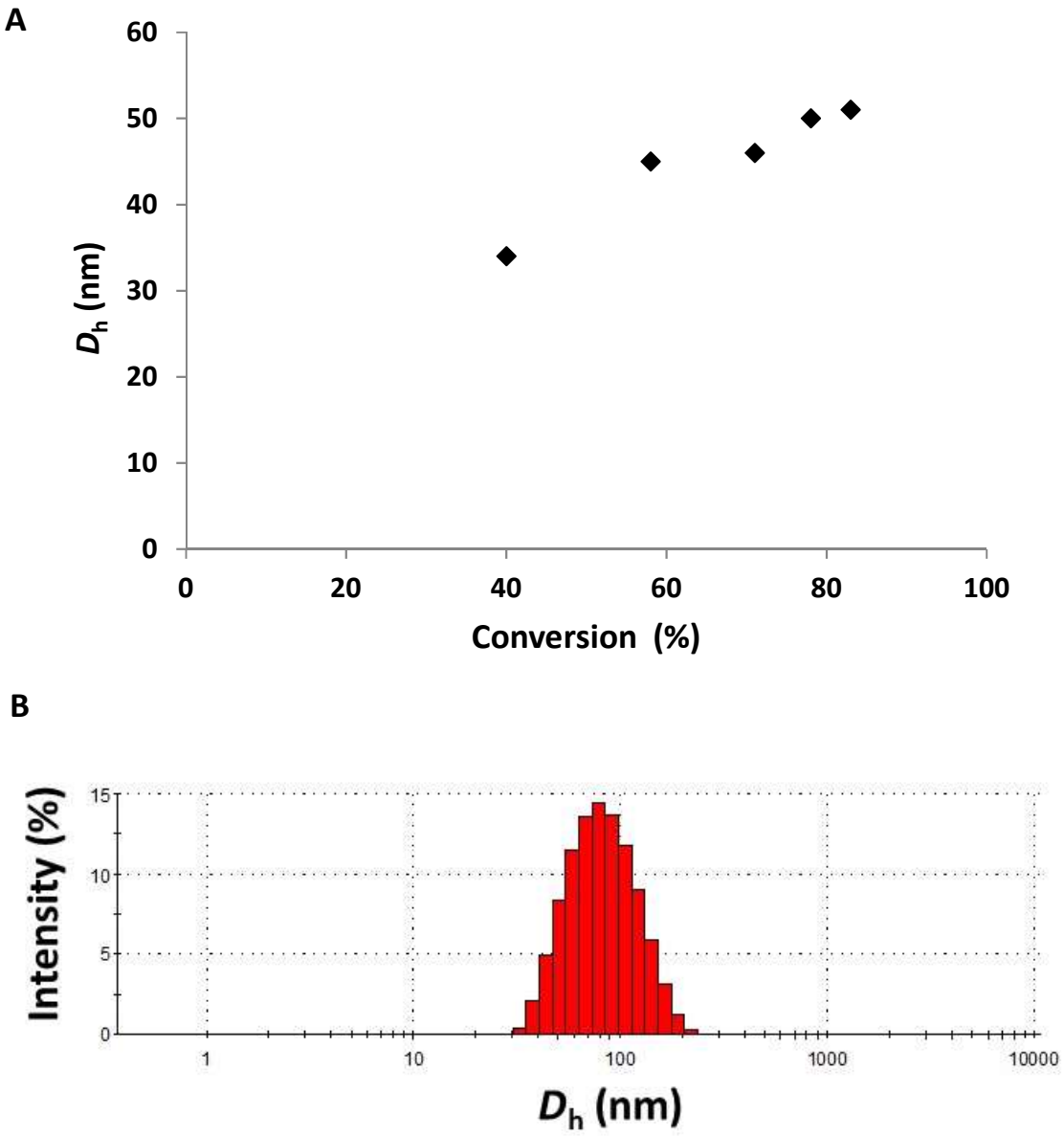

Figure S8. (A) Evolution of the nanoparticle hydrodynamic diameter D_h (determined by QELS) with nBA conversion during PISA-RAFT experiment in water/acetonitrile 50 vol% (Exp. **5** in Table S1). (B) Intensity distribution of the sample (monomer conversion = 83%). Corresponding number distribution is given in Fig. 4.

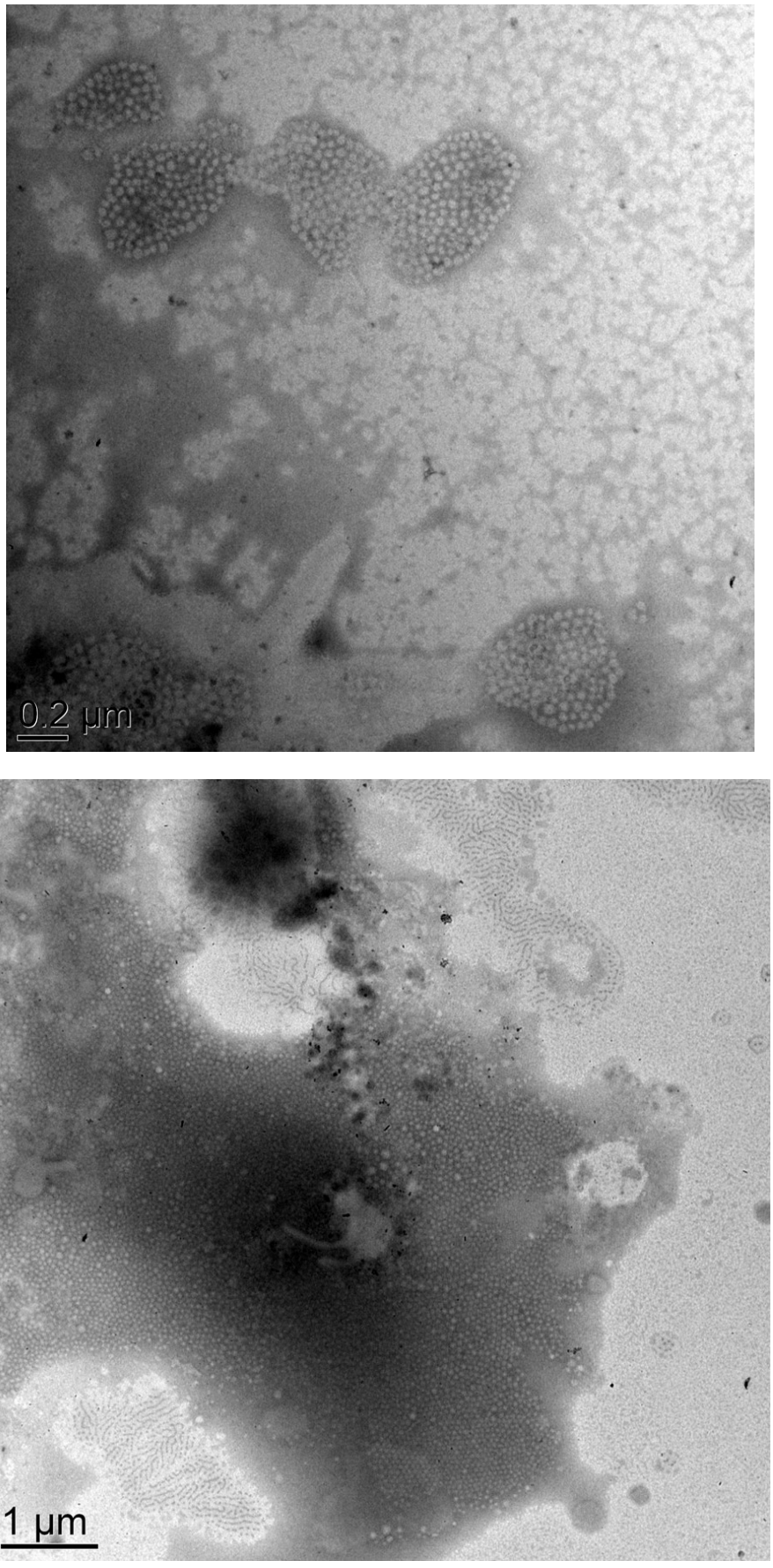

Figure S9. Complementary TEM images of the nanoparticles

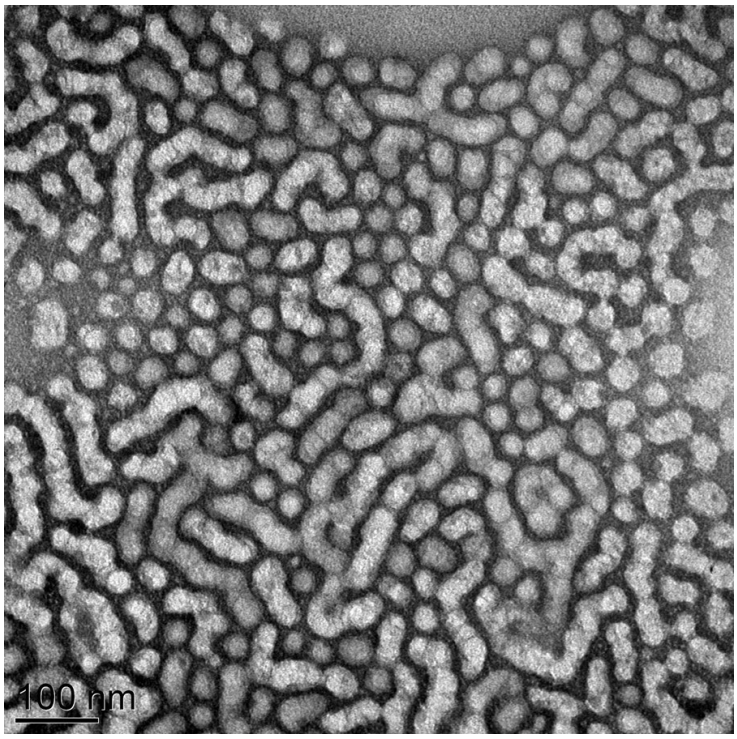

Figure S10. TEM image illustrating the nanoparticle fusion under the electron beam

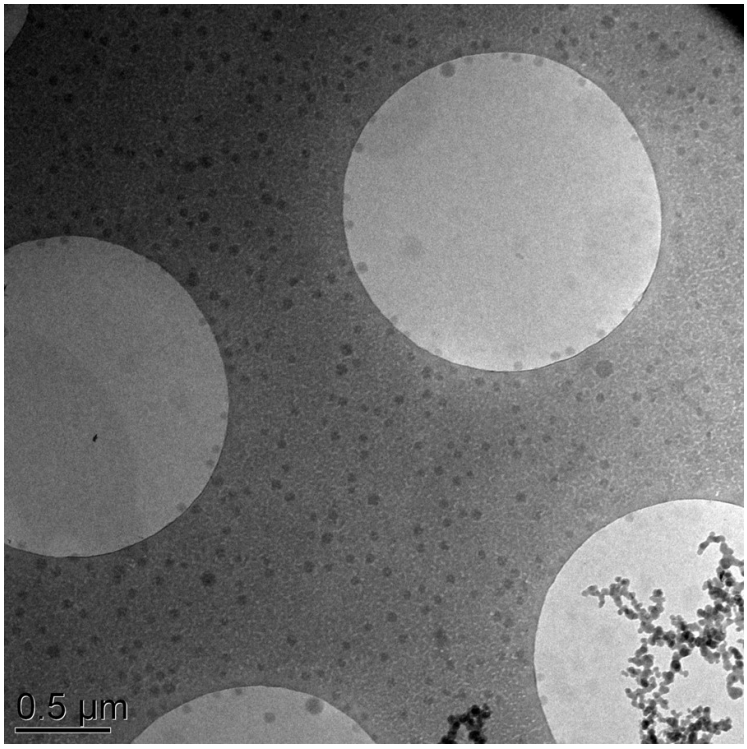

Figure S11. Complementary cryoTEM image showing that the nanoparticles were mainly located on top of the carbon support (dark grey area). Few of them were located on the edge of the holes (light grey areas). Dark crystals like in the bottom right hole corresponded to ice crystals formed during the cryo process.

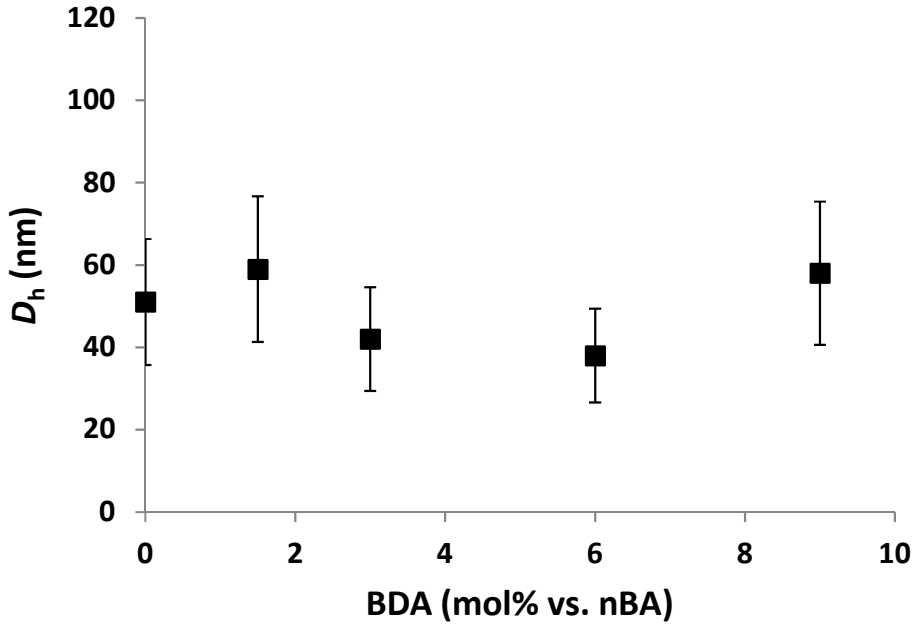

Figure S12. Hydrodynamic diameter (Dh, determined by QELS) of the PISA-RAFT nanoparticles obtained with an increasing molar ratio of BDA crosslinker (Exp. **5-9** in Table S1).

UV-Vis absorption and fluorescence spectra of the fluorescent PISA-RAFT nanoparticles.

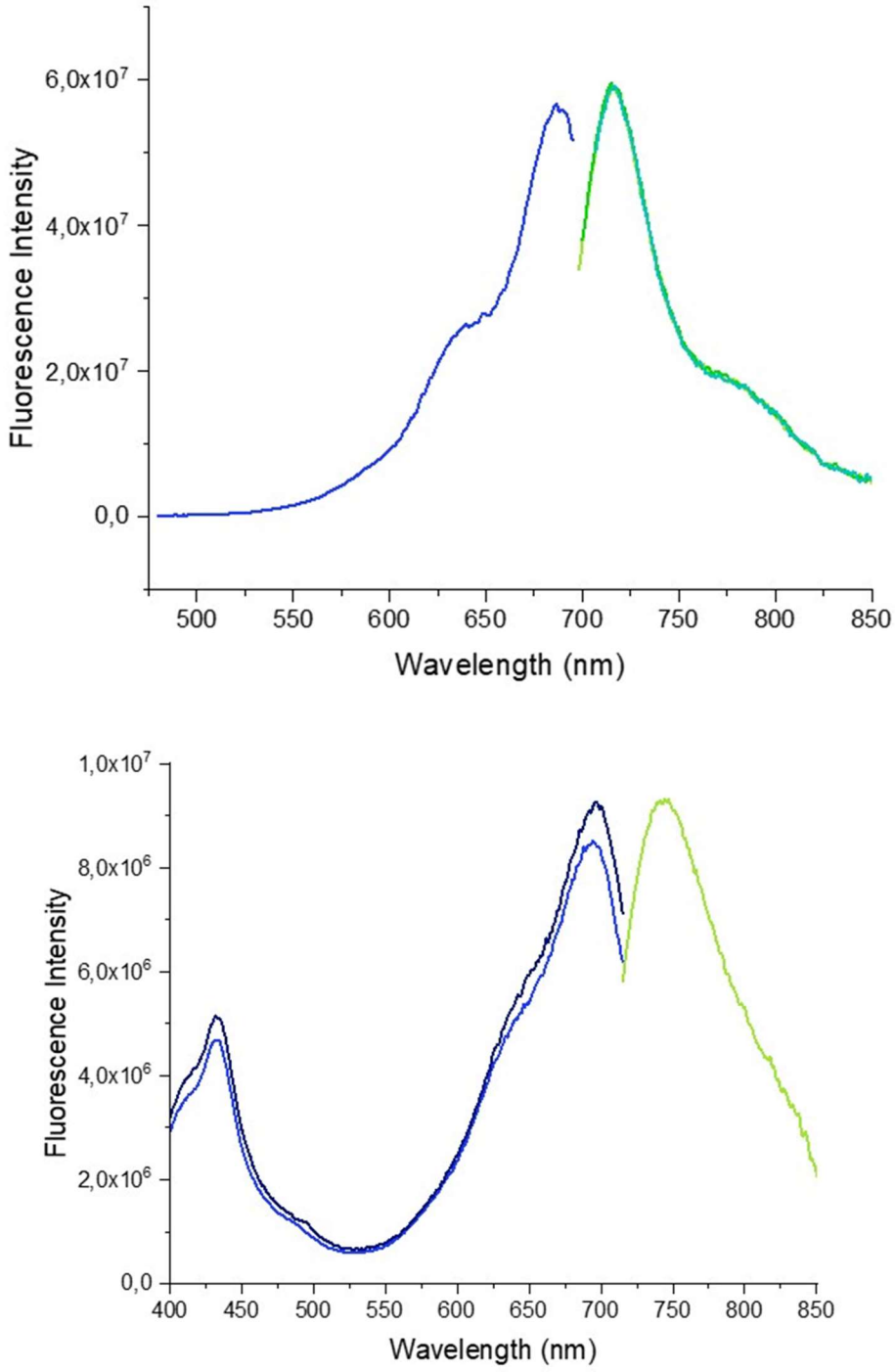

Figure S13. Excitation (blue curves) and emission (green curves) spectra of NIR-fluorescent PISA-RAFT nanoparticles samples. A) Cy5.5-fluorescent nanoparticles excitation spectrum for λ_{em} = 710 nm (blue) and fluorescence emission spectra respectively for λ_{ex} = 683 nm (green) and λ_{ex} = 685 nm (dark green), slits = 1.75 nm in all cases. B) PDI-BisMAm-fluorescent nanoparticles excitation spectra respectively for λ_{em}=730 nm (blue) and λ_{em}=745 nm (dark blue) and fluorescence emission spectrum for λ_{ex}= 695 nm (green), slits = 6 nm in all cases.

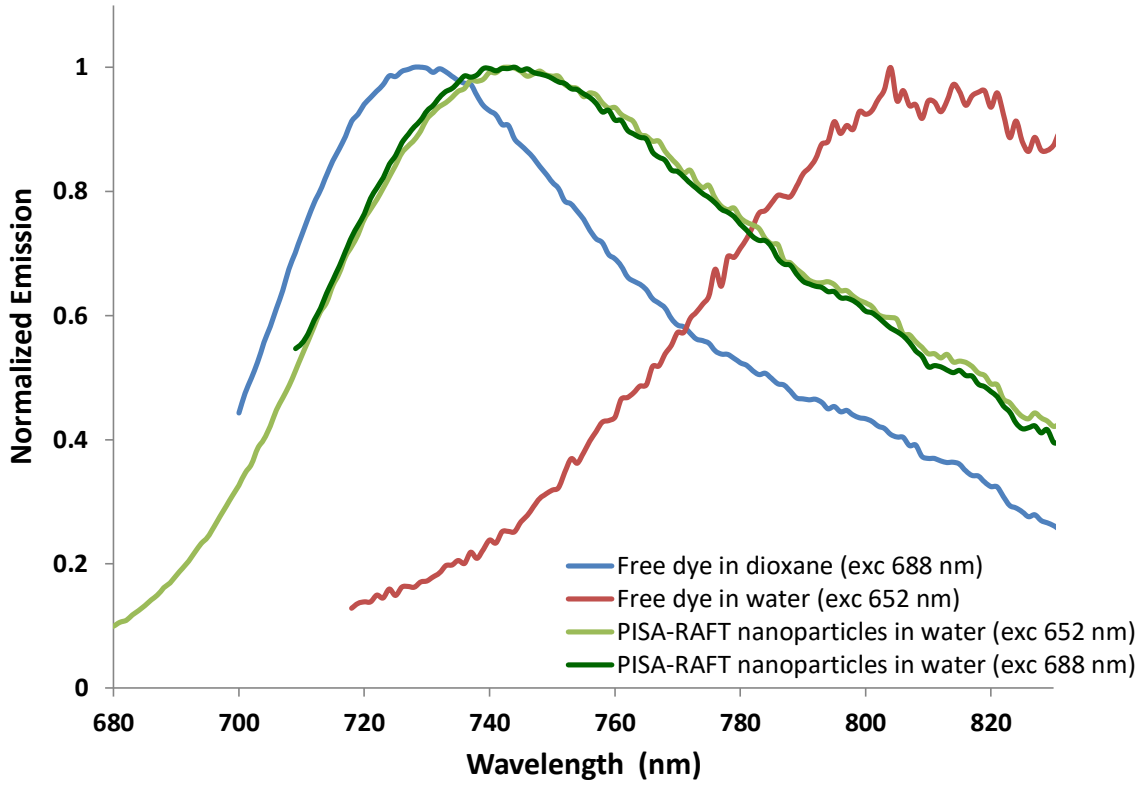

Figure S14. Comparison of the fluorescence emission spectra of the free PDI-BisMAm dye in dioxane (blue) and in water (red) with the fluorescence emission of the PDI-BisMAm fluorescent PISA-RAFT nanoparticles (green).

Calculated nanoparticle characteristics for the reference experiment 5.

Table S3. Input and calculated parameters for the nanoparticles produced in the reference experiment **5** in Table S1.

Input parameters	**Abbreviation**	**Value**
C-C bond length	L_{C-C}	0.154 nm
Avogadro number	N_A	6.02×10^{23} molec.mol^{-1}
PnBA density	d_{PnBA}	1.087 g.cm^{-3}
Initial mass of nBA	m_{nBA_0}	0.36 g
DP_n PNAM macroCTA	$DP_{macroCTA}$	79
Initial mole number of PNAM macroCTA	$n_{macroCTA}$	$1.79.10^{-5}$ mol
nBA final conversion	$Conv_{nBA}$	83 %
D_h (QELS)*	D_h	53 nm
Hydrophobic core diameter (TEM)*	D_{core}	38 nm

* For those indicative estimations, we assumed that the hydrodynamic diameter determined by QELS and the core diameter determined from TEM images are reflective of respectively the overall diameter of the "hairy" nanoparticles and the PnBA core of the nanoparticles

Calculated characteristics	**Abbreviation**	**Equation**	**Values for Exp. 5**
Volume of PnBA core	$V_{PnBA\ core}$	$\frac{4\times\pi}{3}\times\left(\frac{D_{core}}{2}\right)^3$	2.9×10^{-17} cm^3
Mass of PnBA core	$m_{PnBA\ core}$	$V_{PnBA\ core}\times d_{PnBA}$	3.1×10^{-17} g
Total number of nanoparticles (NP)	Nb_{NP}	$\frac{m_{nBA_0}\times\frac{Conv_{nBA}}{100}}{m_{PnBA\ par\ NP}}$	9.6×10^{15}
Theoretical length of a fully extended PNAM macroCTA chain	$L_{macroCTA}$	$2\times L_{C-C}\times\sin\left(\frac{120}{2}\right)\times DP_{macroCTA}$	21 nm
Theoretical maximum NP diameter	$D_{max\ theo}$	$D_{core}+L_{macroCTA}\times2$	80 nm
Number of PNAM macroATC per NP	$Nb_{hairs\ per\ NP}$	$\frac{n_{macroCTA}\times N_A}{Nb_{NP}}$	1125
Surface area of the NP core	S_{core}	$4\times\pi\times\left(\frac{D_{core}}{2}\right)^2$	4536 nm^2
Surface area of the NP outside corona (equivalent sphere)	S_{corona}	$4\times\pi\times\left(\frac{D_h}{2}\right)^2$	8825 nm^2
Number of polymer hairs per nm² of NP core surface	$Nb_{hairs\ per\ core\ surface}$	$\frac{Nb_{hairs\ perNP}}{S_{core}}$	0.25 hair.nm^{-2}
Number of polymer hairs per nm² of NP outside corona surface surface	$Nb_{hairs\ per\ corona\ surface}$	$\frac{Nb_{hairs\ per\ NP}}{S_{corona}}$	0.13 hair.nm^{-2}
Core specific area per hair	$SA_{core\ per\ hair}$	$\frac{S_{core}}{Nb_{hairs\ per\ NP}}$	4 nm^2
Outside corona specific area per hair	$SA_{corona\ per\ hair}$	$\frac{S_{corona}}{Nb_{hairs\ per\ NP}}$	7.9 nm^2
Average distance between two hairs at the NP core surface	$D_{hair-hair\ at\ core}$	$\sqrt{SA_{core\ per\ hair}}$	2 nm
Average distance between two hairs at the NP outside corona surface	$D_{hair-hair\ at\ corona}$	$\sqrt{SA_{corona\ per\ hair}}$	2.8 nm

Calculated nanoparticle characteristics for experiment NP3.

Table S4. Calculated parameters for the nanoparticles produced in experiment **NP3**.

Parameter	Abreviation	Equation	Values for NP3
cRGDcluster-PNAM macroCTA mol% (vs. Total macroCTA)	$Mol\%_{\text{cRGDcluster}}$	$mol\%_{cRGDcluster-PNAM\ macroCTA}$	2.5
Number of PNAM hairs per NP	$Nb_{PNAM\ hairs\ per\ NP}$	$\frac{n_{macroATC} \times (1 - Mol\%_{\text{cRGDcluster}}) \times N_A}{Nb_{NP}}$	1097
Number of cRGDcluster-PNAM hairs per NP	$Nb_{cRGDcluster\ per\ NP}$	$\frac{n_{macroCTA} \times Mol\%_{\text{cRGDcluster}} \times N_A}{Nb_{NP}}$	28
NP core surface area	S_{core}	$4 \times \pi \times \left(\frac{D_{core}}{2}\right)^2$	4536 nm²
NP outside corona surface area	S_{corona}	$4 \times \pi \times \left(\frac{D_h}{2}\right)^2$	8825 nm²
Core specific area per cRGDcluster	$S_{core\ per\ cRGDcluster}$	$\frac{S_{core}}{Nb_{cRGDcluster\ per\ NP}}$	161 nm²
Outside corona specific area per cRGDcluster	$S_{corona\ per\ cRGDcluster}$	$\frac{S_{corona}}{Nb_{cRGDcluster\ per\ NP}}$	314 nm²
Average distance between two cRGDcluster-PNAM hairs at the NP core surface	$D_{cRGDcluster\ hairs\ at\ core}$	$\sqrt{S_{core\ per\ cRGDcluster}}$	12.7 nm
Average distance between two cRGDcluster-PNAM hairs at the NP outside corona surface	$D_{cRGDcluster\ hairs\ at\ corona}$	$\sqrt{S_{corona\ per\ cRGDcluster}}$	17.7 nm
Average number of Cy5.5-Am fluorophores per NP	$Nb_{Cy5.5\ per\ NP}$	$\frac{n_{Cy5.5-Am} \times N_A}{Nb_{NP}}$	265

References.

1. T. Ribeiro, S. Raja, A. S. Rodrigues, F. Fernandes, J. P. S. Farinha and C. Baleizão, *RSC Advances*, 2013, **3**, 9171-9174.
2. A. Favier, C. Ladaviere, M. T. Charreyre and C. Pichot, *Macromolecules*, 2004, **37**, 2026-2034.